JACS
JOURNAL OF THE AMERICAN CHEMICAL SOCIETY

Communication

pubs.acs.org/JACS

Anti-frameshifting Ligand Reduces the Conformational Plasticity of the SARS Virus Pseudoknot

Dustin B. Ritchie,[†] Jingchyuan Soong,[†] William K. A. Sikkema,[‡] and Michael T. Woodside*[,†,‡]

[†]Department of Physics, University of Alberta, Edmonton, Alberta T6G 2E1, Canada

[‡]National Institute for Nanotechnology, National Research Council, Edmonton, Alberta T6G 2M9, Canada

Supporting Information

ABSTRACT: Programmed −1 ribosomal frameshifting (−1 PRF) stimulated by mRNA pseudoknots regulates gene expression in many viruses, making pseudoknots potential targets for anti-viral drugs. The mechanism by which pseudoknots trigger −1 PRF, however, remains controversial, with several competing models. Recent work showed that high −1 PRF efficiency was linked to high pseudoknot conformational plasticity via the formation of alternate conformers. We tested whether pseudoknots bound with an anti-frameshifting ligand exhibited a similar correlation between conformational plasticity and −1 PRF efficiency by measuring the effects of a ligand that was found to inhibit −1 PRF in the SARS coronavirus on the conformational dynamics of the SARS pseudoknot. Using single-molecule force spectroscopy to unfold pseudoknots mechanically, we found that the ligand binding effectively abolished the formation of alternate conformers. This result extends the connection between −1 PRF and conformational dynamics and, moreover, suggests that targeting the conformational dynamics of pseudoknots may be an effective strategy for anti-viral drug design.

Ribosomes synthesize proteins by reading a messenger RNA (mRNA) in 3-nucleotide (nt) steps, maintaining a specific reading frame until a stop codon is reached. In programmed −1 ribosomal frameshifting (−1 PRF), the ribosome skips backward on the mRNA by 1 nt, typically resulting in the bypass of a stop codon and the translation of a new reading frame specifying a different amino acid sequence.[1] Many RNA viruses make use of −1 PRF to produce structural and enzymatic proteins in tightly regulated ratios.[2] For example, the Severe Acute Respiratory Syndrome coronavirus (SARS CoV) uses −1 PRF to regulate production of RNA-dependent RNA polymerase and other replicase proteins.[3] Altering the −1 PRF efficiency can greatly reduce SARS virus infectivity;[4] a similar effect has also been demonstrated for HIV.[2a,b,5] The importance of −1 PRF efficiency to virus replication has motivated efforts to develop new anti-viral therapeutics that target the frameshifting mechanism in viruses such as HIV[6] and SARS.[7]

Frameshifting depends on two specific components in the mRNA: a 7-nt "slippery sequence" at which −1 PRF occurs, and a stimulatory structure, usually a pseudoknot, located 6−8 nt downstream.[1] Efforts to reduce viral infectivity by modulating frameshifting efficiency have primarily focused on identifying small molecules that bind to the stimulatory structures or developing anti-sense oligonucleotides to alter them. Small molecules that modulate frameshifting efficiencies for SARS CoV[7] and HIV-1[6] have indeed been found, but interpreting the effects of such molecules can be complicated. The mechanism of binding is not always known, nor are the effects of binding on the stability and structure of the stimulatory RNA, and the interactions with the stimulatory RNA may not be specific. Most importantly, the mechanisms by which the compounds regulate −1 PRF are unclear. For example, some compounds with promise against HIV-1 likely bind RNA in general, rather than specific stimulatory structures, suggesting that they may modulate −1 PRF efficiency via interactions with ribosomal RNA.[6,8]

A complicating factor in efforts to develop drugs that target frameshifting is the fact that the mechanism of −1 PRF is still incompletely understood, especially the role of the stimulatory structure in determining −1 PRF efficiency. Models have been proposed with −1 PRF occurring at various steps in the elongation cycle.[1,9] The tension generated in the mRNA as the ribosome unwinds the stimulatory structure plays a key role in several of these models. For example, one commonly cited model posits that the pseudoknot acts as a mechanical roadblock to ribosome translocation, weakening the codon/anticodon base-pairing when the ribosome is over the slippery sequence, thereby promoting a −1 shift in reading frame.[9d,10] Direct measurements of translocating ribosomes do show that tension in the transfer RNA (tRNA)-mRNA linkage is used by the ribosome to promote unwinding of structured RNAs at the mRNA entry site.[11] However, −1 PRF efficiency is not determined by the thermodynamic stability of pseudoknots,[12] nor is it correlated with pseudoknot-induced ribosomal pausing[10] as would be expected from this picture. Early studies using mechanical tension to mimic how the ribosome unwinds RNA structure suggested a correlation with resistance to mechanical unfolding,[13] but recently a more comprehensive survey of pseudoknot unfolding showed that −1 PRF efficiency was not, in fact, determined by any characteristic of the mechanical unfolding.[14] Instead, −1 PRF efficiency was unexpectedly found to correlate with the conformational plasticity of the pseudoknot, as reflected in its ability to form alternate structures.

These results suggest that searching for drugs that alter the stability of stimulatory structures may not be an effective strategy. To confirm the notion that pseudoknot conformational plasticity

Received: May 15, 2013
Revised: October 15, 2013
Published: January 21, 2014

dx.doi.org/10.1021/ja410344b | J. Am. Chem. Soc. 2014, 136, 2196−2199

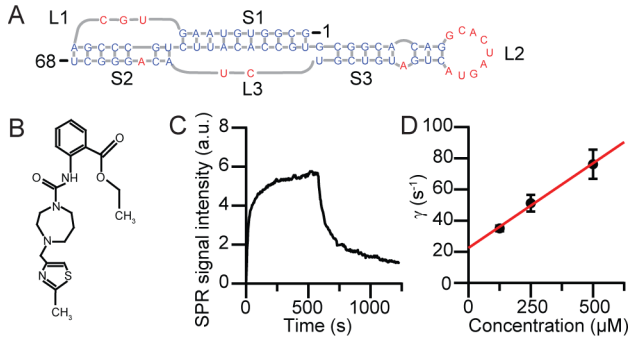

Figure 1. (a) SARS CoV pseudoknot, consisting of three stems (S1−S3) and three loops (L1−L3), indicated on the secondary structure. Base-pairs are shown in blue, unpaired nucleotides in red. (b) Structure of the ligand MTDB. (c) The SPR signal rose exponentially upon addition of MTDB to immobilized RNA. (d) Dependence of the signal rise rate γ on the ligand concentration, yielding K_d = 210±20 μM.

is a factor determining −1 PRF efficiency and test whether it provides a useful basis for designing anti-frameshifting drugs, we focused on the binding of an anti-frameshifting ligand to the SARS CoV pseudoknot. The SARS CoV pseudoknot has an unusual three-stemmed structure (Figure 1a),[15] in contrast to the two-stemmed hairpin-type pseudoknots more commonly employed by viruses to stimulate −1 PRF.[1a] Recently, *in silico* screening for compounds that bind the SARS CoV pseudoknot found a small molecule, 2-{[4-(2-methylthiazol-4-ylmethyl)-[1,4]diazepane-1-carbonyl]amino}benzoic acid ethyl ester (MTDB, Figure 1b), that suppresses −1 PRF in both cell-free and cellular translation systems.[7a] The effect was specific to the SARS pseudoknot, as no reduction in −1 PRF was observed for two other pseudoknots tested as negative controls.

We first measured the binding affinity of MTDB to the SARS CoV pseudoknot using surface plasmon resonance (SPR). RNA consisting of the 68-nt pseudoknot sequence with an 11-nt 5′ single-stranded (ss) overhang was bound to complementary ssDNA immobilized on a gold surface (see Supporting Information for details). The SPR signal intensity rise upon addition of ligand (Figure 1c) was fit by a single exponential, allowing the apparent dissociation constant, K_d, to be found from the dependence of the signal rise rate, γ, on the ligand concentration (Figure 1d). The result was K_d = 210±20 μM. Due to its low affinity for pseudoknot binding, this compound is likely not a good drug candidate, but it is nevertheless both effective at suppressing −1 PRF and specific to the SARS pseudoknot, making it well-suited for this study.

The effect of MTDB binding on the mechanical stability and structural dynamics of the SARS CoV pseudoknot was tested using optical tweezers. RNA containing the pseudoknot sequence flanked on each side by kilobase-long "handle" sequences was transcribed *in vitro*, annealed to ssDNA complementary to the handles, and attached to beads held in optical traps (Figure 2a, inset), as described previously.[14] The RNA was held near zero force for 3 s in 50 mM MOPS, pH 7.0, 130 mM KCl, 4 mM $MgCl_2$, 0.3% DMSO to permit folding and ligand binding, and then the traps were separated at constant velocity to apply force while measuring molecular extension, thereby generating force/extension curves (FECs) (Figure 2a). Characteristically, the force in the FECs rises nonlinearly with extension as the handles are stretched, until there is an abrupt extension increase and concomitant force decrease when the structure unfolds.[16] With or without ligand present, unfolding

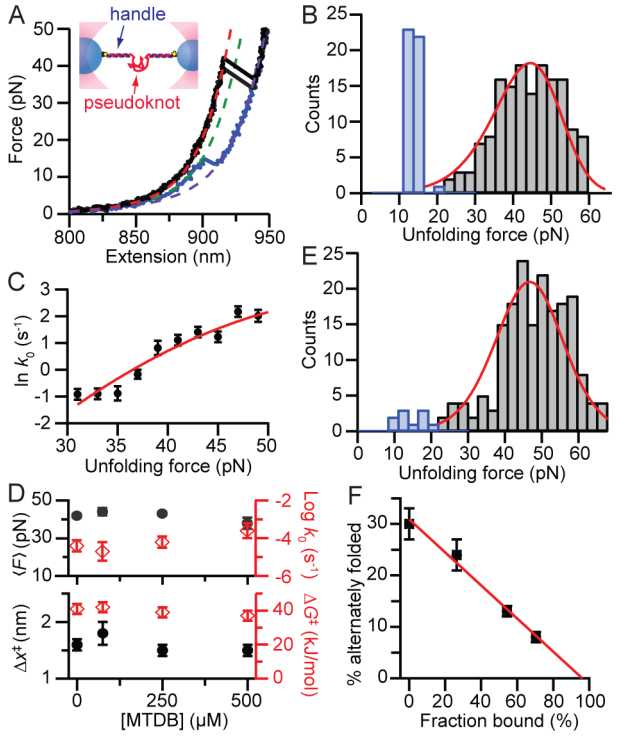

Figure 2. (a) A single SARS CoV pseudoknot molecule tethered between two beads held in optical traps (inset). The RNA contour length changes abruptly upon unfolding, causing a "rip" in the FEC. Most FECs showed a length change, found from WLC fits to Eqn S1 (dashed lines), consistent with the native structure (black), but some (blue) revealed a smaller, alternate structure. (b) Fit of the distribution of unfolding forces for the native pseudoknot in the absence of ligand (black) to Eqn S2 to determine the energy landscape parameters for mechanical unfolding. The alternate structure unfolded at a significantly lower force (blue). (c) Fit of the force-dependent unfolding rate to Eqn S3. (d) Average unfolding force (upper panel, black) and zero-force unfolding rate (upper panel, red), as well as the position (lower panel, black) and height of the barrier for unfolding. All were unchanged by ligand binding. (e) Unfolding force distribution in the presence of 250 μM ligand, showing a reduction in the extent of alternate structure formation. (f) The extent of alternate structure formation dropped linearly with the fraction of pseudoknots that were bound by ligand.

occurred most commonly as a two-state process without intermediates (Figure 2a, black). The change in contour length during such unfolding events, ΔL_c, was found by fitting the folded and unfolded branches of the FECs (Figure 2a, red and purple, respectively) to two extensible wormlike chains (WLCs, see Eqn S1 in the Supporting Information) in series, one for the handles and one for the unfolded RNA.[14] The result, ΔL_c = 33±1 nm (all errors represent standard error on the mean), agrees well with the value 34 nm expected from the predicted secondary structure,[15a,b] assuming an end-to-end distance in the folded structure of 6 nm similar to the infectious bronchitis virus pseudoknot[17] and consistent with the tertiary structure proposed from computational work.[7a] The pseudoknot was thus natively folded in these curves. However, without ligand present, a substantial minority (30±3%) of the curves displayed unfolding at a lower force and with an unexpectedly short ΔL_c, 21±1 nm, indicating that the pseudoknot was folded into an alternate structure at the start of those pulls (Figure 2a, blue; WLC fit, green). The distributions of ΔL_c and unfolding force suggest only a single alternate conformation is present. Increasing the waiting time between pulls to 10 s did not change the extent of alternate

dx.doi.org/10.1021/ja410344b | J. Am. Chem. Soc. 2014, 136, 2196−2199

structure formation noticeably, suggesting that any interconversion between the structures is very slow.

We quantified the resistance of the pseudoknot to mechanical unfolding from the distribution of unfolding forces, $p(F)$ (Figure 2b). The average unfolding force for the native structure without ligand bound was 42±1 pN. Additionally, the height of the energy barrier for unfolding, $\Delta G^{\ddagger}$, the distance to the barrier from the folded state, $\Delta x^{\ddagger}$, and the unfolding rate at zero force, k_0, were found by fitting $p(F)$ to a kinetic theory for unfolding based on a one-dimensional model of the energy landscape (Eqn S2).[18] A complementary analysis based on the cumulative probability of unfolding[19] yielded the unfolding rate as a function of force, which was well fit by Eqn S3 (Figure 2c). Data were analyzed by both methods and the results averaged, yielding $\log k_0 = -4.4\pm0.3\ s^{-1}$, $\Delta x^{\ddagger} = 1.6\pm0.1$ nm, and $\Delta G^{\ddagger} = 41\pm3$ kJ/mol for the pseudoknot without ligand.

We repeated these measurements with three concentrations of MTDB: 75, 250, and 500 μM. Qualitatively, the behavior of the pseudoknot was similar in all cases; there were no additional subpopulations in the pulling curves, such as curves in which the RNA did not unfold (a possible result of covalent cross-linking by the ligand) or refold (a possible result of binding to the unfolded RNA). The average unfolding force and landscape parameters for the native structure were found to remain the same, within error; any changes were too subtle to detect (Figure 2d, Table S1). Hence, the ligand did not significantly change the mechanical stability of the pseudoknot. Note that the weak binding revealed by SPR would be expected to lead to only a small increase in the unfolding force: $K_d = 210$ μM implies a stabilization energy of 21 kJ/mol. Given $\Delta L_c = 33$ nm upon unfolding, the force should increase at equilibrium by only 1−2 pN, within the margin of the experimental uncertainty and thus too small to detect. The average force for unfolding the alternate structure (∼16 pN) was also unchanged within error, as was the ΔL_c for the alternate structure (all results listed in Table S1).

However, the fraction of FECs showing unfolding from the alternate structure was progressively reduced at increasing ligand concentrations, from 30±3% without ligand to 8±1% at 500 μM. Representative unfolding force distributions are shown in Figure 2e at 250 μM MTDB, for the native (black) and alternate (blue) structures. Inferring from K_d the fraction of ligand-bound pseudoknots, we found that the prevalence of the alternate structure varied linearly with the fraction of pseudoknot bound (Figure 2f). The incidence of alternate structures goes to zero when 96±8% pseudoknots are bound, indicating that ligand binding effectively eliminates the formation of alternate structures. This reduction in alternate structure formation mirrors the suppression of −1 PRF efficiency caused by the ligand, which was found to reduce −1 PRF to near-background levels.[7a]

A model for MTDB binding to the SARS pseudoknot was proposed previously based on docking calculations.[7a] In this model, MTDB forms H-bonds with nucleotides in loop 3, which bridges the junction between stems 2 and 3 (Figure 1a). Only a few bonds to the RNA were proposed in the model, consistent with the relatively weak binding we found. Interestingly, the junction where binding is thought to occur contains nucleotides that are susceptible to cleavage by probes sensitive to both double- and single-stranded RNA, indicating that the junction is flexible and exists in a dynamic conformational equilibrium.[15b] Such a picture is also consistent with our results, which suggest that MTDB binds to a flexible region of the SARS pseudoknot, thereby stabilizing it conformationally. Analogous behavior is seen in riboswitches, where ligand binding greatly reduces the conformational flexibility of the RNA,[20] although in the case of riboswitches the ligand binding usually enhances the mechanical stability of the structure significantly, as well.[21] A crucial contrast here is that the ligand does not significantly increase the mechanical stability of the pseudoknot structure. Indeed, the observation that a pseudoknot-binding ligand that suppresses −1 PRF does not significantly alter the mechanical stability of the pseudoknot, but does suppress its ability to sample multiple structures, provides further evidence against the view that pseudoknot mechanical stability determines −1 PRF efficiency.[13] Instead, it reinforces the notion that the conformational plasticity and dynamic characteristics of the pseudoknot play an important role.[14,22] We thus propose a mechanism whereby MTDB binding reduces −1 PRF efficiency by reducing the conformational plasticity of the pseudoknot, consistent with our previous work highlighting an under-appreciated role for pseudoknot structural dynamics in regulating −1 PRF levels.[14]

How might pseudoknot structural dynamics help determine −1 PRF efficiency? The ribosome actively generates tension in the mRNA as structure is unfolded,[11] suggesting that a dynamic conformational equilibrium could cause fluctuations in this tension which, when communicated to the tRNA-mRNA complex, lead to a frameshift.[14] This picture is consistent with a previous proposal that refolding of a partially unfolded pseudoknot during accommodation might induce a frameshift by pulling back on the mRNA.[9c] It is also supported by evidence of dynamic structural fluctuations in pseudoknots that stimulate −1 PRF efficiently: pseudoknot structures with a relatively high frequency of base-pair breathing at the junction of the two stems have been found to be more efficient −1 PRF stimulators than more conformationally rigid pseudoknots.[22a]

Given the many elements involved in −1 PRF, MTDB could also modulate frameshifting through effects other than changes in the pseudoknot structural dynamics. For example, the ribosome interacts with the pseudoknot during frameshifting in a variety of ways, which might be affected by MTDB binding. Structural and functional studies suggest that triplex structures and exposed loop nucleotides may make or direct specific contacts to the ribosome that affect −1 PRF efficiency, possibly explaining why the efficiency can be reduced by removing or altering these structures.[12b,13a,23] MTDB binding might prevent such specific interactions needed to promote −1 PRF via protection, steric clash, or stabilization of a nonfunctional pseudoknotted conformation, or it might create new interactions leading to increased proofreading. The ribosomal helicase also interacts generically with the mRNA structures it unwinds, to facilitate the melting process,[11] possibly biasing the dynamic equilibrium in favor of certain structures or speeding up equilibration rates. MTDB binding to the pseudoknot might modulate the interactions mediating this active unwinding of mRNA structure, thereby affecting the coupling of structural dynamics and interactions with the ribosome that are important for regulating −1 PRF efficiency.

However, the fact that −1 PRF efficiency is correlated with conformational plasticity when varying two completely independent aspects of the measurement (anti-frameshifting ligand binding, in contrast to identity of the pseudoknot used to stimulate frameshifting[14]) is highly suggestive that the correlation reflects an actual mechanistic feature of −1 PRF common to all the measurements, rather than some artifact. Moreover, using ligand binding to alter −1 PRF efficiency as we have done here, as opposed to making mutations in the

pseudoknot[12b,13a,23] or comparing pseudoknots from different species,[14] allows a more controlled study of the relationship between these structures and −1 PRF efficiency, since comparisons can be made for identical RNA molecules. It is interesting to note that one of the challenges in building models of −1 PRF has been reconciling, within a single mechanistic framework, the seemingly disparate characteristics that appear to play important roles during frameshifting. While much work remains before a complete model of −1 PRF can be realized, the observation of a correlation between −1 PRF efficiency and formation of alternate conformations across an increasing range of conditions suggests that conformational plasticity may be a common feature linking various frameshift signals, highlighting its importance as a determinant of −1 PRF efficiency.

The role of mRNA conformational plasticity in −1 PRF could be probed further by extending this kind of study to other stimulatory structures. For example, in the case of HIV-1, −1 PRF is apparently stimulated by a hairpin with a 3-nt bulge.[24] The local stability of the three base-pairs adjacent to the mRNA entry tunnel is known to influence −1 PRF efficiency,[25] but the structural dynamics of the hairpin have yet to be explored as a determining factor. Furthermore, the HIV-1 stimulatory structure may actually form an intramolecular triplex during −1 PRF,[26] raising structural parallels with pseudoknot-induced frameshifting. Ligands that modulate −1 PRF efficiency in HIV-1[6,8] would provide an opportunity to probe the link between conformational dynamics and −1 PRF in a different system and thereby test the generality of the proposed mechanism.

Finally, we note that our results suggest that when screening for molecules with potential as anti-viral therapeutics that work by modulating −1 PRF efficiency, focusing on the effects of compounds on pseudoknot conformational dynamics should prove more fruitful than focusing simply on modulating the stability of the pseudoknot structure. A similar strategy may also prove effective for targeting −1 PRF stimulated by other types of structures, like the hairpin in the HIV-1 frameshift signal.

■ ASSOCIATED CONTENT

Supporting Information

Materials and methods, Eqns S1−S3, and Table S1. This material is available free of charge via the Internet at http://pubs.acs.org.

■ AUTHOR INFORMATION

Corresponding Author

michael.woodside@ualberta.ca

Notes

The authors declare no competing financial interest.

■ ACKNOWLEDGMENTS

This work was supported by Alberta Innovates Technology Futures, the National Institute for Nanotechnology, and the Natural Sciences and Engineering Research Council of Canada. We thank Lars Laurentius for assistance with SPR.

■ REFERENCES

(1) (a) Giedroc, D. P.; Cornish, P. V. *Virus Res.* **2009**, *139*, 193. (b) Brierley, I.; Gilbert, R. J. C.; Pennell, S. *Nucleic Acids Mol. Biol.* **2010**, *24*, 149.

(2) (a) Dulude, D.; Berchiche, Y. A.; Gendron, K.; Brakier-Gingras, L.; Heveker, N. *Virology* **2006**, *345*, 127. (b) Telenti, A.; Martinez, R.; Munoz, M.; Bleiber, G.; Greub, G.; Sanglard, D.; Peters, S. *J. Virol.* **2002**, *76*, 7868. (c) Dinman, J. D.; Wickner, R. B. *J. Virol.* **1992**, *66*, 3669.

(3) Thiel, V.; Ivanov, K. A.; Putics, A.; Hertzig, T.; Schelle, B.; Bayer, S.; Weissbrich, B.; Snijder, E. J.; Rabenau, H.; Doerr, H. W.; Gorbalenya, A. E.; Ziebuhr, J. *J. Gen. Virol.* **2003**, *84*, 2305.

(4) (a) Plant, E. P.; Rakauskaite, R.; Taylor, D. R.; Dinman, J. D. *J. Virol.* **2010**, *84*, 4330. (b) Plant, E. P.; Sims, A. C.; Baric, R. S.; Dinman, J. D.; Taylor, D. R. *Viruses* **2013**, *5*, 279.

(5) Shehu-Xhilaga, M.; Crowe, S. M.; Mak, J. *J. Virol.* **2001**, *75*, 1834.

(6) Brakier-Gingras, L.; Charbonneau, J.; Butcher, S. E. *Exp. Opin. Ther. Targets* **2012**, *16*, 249.

(7) (a) Park, S. J.; Kim, Y. G.; Park, H. J. *J. Am. Chem. Soc.* **2011**, *133*, 10094. (b) Ahn, D. G.; Lee, W.; Choi, J. K.; Kim, S. J.; Plant, E. P.; Almazán, F.; Taylor, D. R.; Enjuanes, L.; Oh, J. W. *Antiviral Res.* **2011**, *91*, 1.

(8) Marcheschi, R. J.; Tonelli, M.; Kumar, A.; Butcher, S. E. *ACS Chem. Biol.* **2011**, *6*, 857.

(9) (a) Jacks, T.; Madhani, H. D.; Masiarz, F. R.; Varmus, H. E. *Cell* **1988**, *55*, 447. (b) Plant, E. P.; Jacobs, K. L.; Harger, J. W.; Meskauskas, A.; Jacobs, J. L.; Baxter, J. L.; Petrov, A. N.; Dinman, J. D. *RNA* **2003**, *9*, 168. (c) Plant, E. P.; Dinman, J. D. *Nucleic Acids Res.* **2005**, *33*, 1825. (d) Namy, O.; Moran, S. J.; Stuart, D. I.; Gilbert, R. J.; Brierley, I. *Nature* **2006**, *441*, 244.

(10) Kontos, H.; Napthine, S.; Brierley, I. *Mol. Cell. Biol.* **2001**, *21*, 8657.

(11) Qu, X.; Wen, J. D.; Lancaster, L.; Noller, H. F.; Bustamante, C.; Tinoco, I. *Nature* **2011**, *475*, 118.

(12) (a) Napthine, S.; Liphardt, J.; Bloys, A.; Routledge, S.; Brierley, I. *J. Mol. Biol.* **1999**, *288*, 305. (b) Chen, X.; Chamorro, M.; Lee, S. I.; Shen, L. X.; Hines, J. V.; Tinoco, I., Jr.; Varmus, H. E. *EMBO J.* **1995**, *14*, 842. (c) Kang, H.; Hines, J. V.; Tinoco, I., Jr. *J. Mol. Biol.* **1996**, *259*, 135.

(13) (a) Chen, G.; Chang, K. Y.; Chou, M. Y.; Bustamante, C.; Tinoco, I., Jr. *Proc. Natl. Acad. Sci. U.S.A.* **2009**, *106*, 12706. (b) Hansen, T. M.; Reihani, S. N.; Oddershede, L. B.; Sørensen, M. A. *Proc. Natl. Acad. Sci. U.S.A.* **2007**, *104*, 5830.

(14) Ritchie, D. B.; Foster, D. A.; Woodside, M. T. *Proc. Natl. Acad. Sci. U.S.A.* **2012**, *109*, 16167.

(15) (a) Plant, E. P.; Pérez-Alvarado, G. C.; Jacobs, J. L.; Mukhopadhyay, B.; Hennig, M.; Dinman, J. D. *PLoS Biol.* **2005**, *3*, e172. (b) Su, M. C.; Chang, C. T.; Chu, C. H.; Tsai, C. H.; Chang, K. Y. *Nucleic Acids Res.* **2005**, *33*, 4265. (c) Baranov, P. V.; Henderson, C. M.; Anderson, C. B.; Gesteland, R. F.; Atkins, J. F.; Howard, M. T. *Virology* **2005**, *332*, 498.

(16) Woodside, M. T.; García-García, C.; Block, S. M. *Curr. Opin. Chem. Biol.* **2008**, *12*, 640.

(17) Green, L.; Kim, C. H.; Bustamante, C.; Tinoco, I., Jr. *J. Mol. Biol.* **2008**, *375*, 511.

(18) Dudko, O. K.; Hummer, G.; Szabo, A. *Phys. Rev. Lett.* **2006**, *96*, 108101.

(19) Dudko, O. K.; Hummer, G.; Szabo, A. *Proc. Natl. Acad. Sci. U.S.A.* **2008**, *105*, 15755.

(20) Serganov, A.; Patel, D. J. *Annu. Rev. Biophys.* **2012**, *41*, 343.

(21) (a) Greenleaf, W. J.; Frieda, K. L.; Foster, D. A. N.; Woodside, M. T.; Block, S. M. *Science* **2008**, *319*, 630. (b) Neupane, K.; Yu, H.; Foster, D. A. N.; Wang, F.; Woodside, M. T. *Nucleic Acids Res.* **2011**, *39*, 7677.

(22) (a) Wang, Y.; Wills, N. M.; Du, Z.; Rangan, A.; Atkins, J. F.; Gesteland, R. F.; Hoffman, D. W. *RNA* **2002**, *8*, 981. (b) Houck-Loomis, B.; Durney, M. A.; Salguero, C.; Shankar, N.; Nagle, J. M.; Goff, S. P.; D'Souza, V. M. *Nature* **2011**, *480*, 561.

(23) (a) Kim, Y. G.; Su, L.; Maas, S.; O'Neill, A.; Rich, A. *Proc. Natl. Acad. Sci. U.S.A.* **1999**, *96*, 14234. (b) Cornish, P. V.; Hennig, M.; Giedroc, D. P. *Proc. Natl. Acad. Sci. U.S.A.* **2005**, *102*, 12694. (c) Olsthoorn, R. C.; Reumerman, R.; Hilbers, C. W.; Pleij, C. W.; Heus, H. A. *Nucleic Acids Res.* **2010**, *38*, 7665. (d) Shen, L. X.; Tinoco, I., Jr. *J. Mol. Biol.* **1995**, *247*, 963. (e) Liphardt, J.; Napthine, S.; Kontos, H.; Brierley, I. *J. Mol. Biol.* **1999**, *288*, 321.

(24) Staple, D. W.; Butcher, S. E. *J. Mol. Biol.* **2005**, *349*, 1011.

(25) Mouzakis, K. D.; Lang, A. L.; Vander Meulen, K. A.; Easterday, P. D.; Butcher, S. E. *Nucleic Acids Res.* **2013**, *41*, 1901.

(26) Dinman, J. D.; Richter, S.; Plant, E. P.; Taylor, R. C.; Hammell, A. B.; Rana, T. M. *Proc. Natl. Acad. Sci. U.S.A.* **2002**, *99*, 5331.